

MR-damped Vehicle Suspension Ride Comfort Enhancement Based on Advanced Proportional-Integral-Differential Sliding Mode Control

Ahmed O. Bashir, Xiaoting Rui, Laith K. Abbas, Qinbo Zhou

Institute of Launch Dynamics, Nanjing University of Science and Technology, Nanjing 210094, P R China, (e-mail: mecheng5120@yahoo.com, ruixt@163.net (Corresponding author), laithabbass@yahoo.com, zqb912_new@163.com)

Abstract: This paper presents advanced proportional-integral-differential sliding mode control (a-PIDSMC) for semi-active vehicle suspension system integrated magnetorheological (MR) fluid damper to improve vehicle ride comfort and stability. The proposed approach consists of a system controller based on a-PIDSMC to compute the desired damping force. The system controller contains two sub-components: (i) a proportional-integral-differential part for disturbance compensation, and (ii) a sliding mode part for executing disturbance estimation errors. Another controller is a continuous state controller which estimates the command voltage that is needed to track the desired damping force. Dynamic model of quarter vehicle suspension system is presented and simulated using Matlab/Simulink software. The results of the proposed a-PIDSMC controlled system are compared with conventional sliding mode controller (SMC), conventional PID controller and the passive suspension system. The performance criteria are evaluated in time domain using two types of road excitation. The simulated results indicate that the proposed controller offers a significant improvement in vehicle ride quality and stability.

Keywords: Vehicle suspension, MR damper, a-PIDSMC control, Ride comfort.

1. INTRODUCTION

Several amounts of research activities have been directed to the suspension system to improve the ride comfort, especially over the last decade. To isolate the body from road and inertial disturbances associated with braking; these disturbances should be absorbed by ideal suspension system (Wright, 1984). Furthermore, suspension system must guarantee less vertical force transmitted to the driver. These goals can be achieved by minimizing the vertical car body acceleration. Moreover, to maximize safety in various driving conditions the optimal contact between road surface and wheel is necessary (Lin and Kanellakopoulos, 1995).

The passive suspension is one of the choices for a vehicle suspension system and has been widely used due to their lower price, simpler structure and simplicity to implementation. However, such suspension elements are passive in nature in the sense that, once implemented, the suspension system cannot adapt to the variety of road surface on which it must operate.

To overcome the above problem, semi-active suspension system is the alternative. In early semi-active suspension system, the regulating of the damping force can be achieved by utilizing the controlled dampers under closed loop control, where it has the potentiality to energy dissipation (Williams, 1994). Semi-active suspension incorporating MR damper, have been used in a wide range of applications in the field of vibration control: from automobiles (Karkoub and Zribi, 2006) to railway vehicles (Liao and Wang, 2003) and civil

constructions such as buildings (Dyke et al., 1996). Thus semi-active with MR-damper becomes one of the most attractive techniques for improving the performance of handling stability and ride comfort of road vehicle.

Magnetorheological fluid damper is a semi active control device, the force produced by the device cannot be adapted directly; only the command voltage applied to the current driver of the MR fluid damper can be controlled straightaway. It has many distinct advantages such as simple structure, small size, fast response, low energy consumption, and continuously controllable resistance (Zhu et al., 2011). However, there are strongly nonlinearity and modelling uncertainties for MR-damper, which may complicate the development of high-performance controllers for MR-damped suspension structure (Yao et al., 2014). In general, the simplicity, applicability and robustness of controllers are designer's targets in industry to have a successful implementation of their controllers. The performance of semi-active suspension systems bets on real-time control schemes.

To controlling MR-damped semi-active suspension system, in addition to a system controller that calculates the desired damping force, a damper controller is also required. The damper controller determines the voltage supplied to the damper such that its actual force tracks the desired force. Various control strategies have been introduced and assessed for the system controller in the past years to improve the dynamics of nonlinear and uncertain suspension systems such as; fuzzy control (Shehata et al., 2015), neural network

control (Guo et al., 2004), fuzzy-PID control (Yang et al., 2011), Genetic PID control (Gad et al., 2015), adaptive neuro-fuzzy hybrid control (Nugroho et al., 2014) and hybrid fuzzy and fuzzy-PID control (Hu et al., 2017). On the other hand, optimization of PID tuning parameters based on Biogeography is reported by (Rajagopal and Ponnusamy, 2014). The drawbacks of such methods lie in the nature of their tuning and the inability to address robustness guarantees. In recent years, several literatures have been covered in the domain of sliding mode control (SMC), and have focused on the improvement for conventional SMC, whereas, they hardly achieved proper performance. The reason for the popularly use of the conventional SMC is the robust-ness of the modelling errors as well as its insensitivity of the parameter variations and extraneous disturbances (Kaya, 2007). Nevertheless, in practical applications, chattering is the disadvantage of a purely design of SMC, which is a high-frequency variation of the control input due to presence of un-modelled dynamics of the system. Chattering could be avoided because, it has harmful effect for the mechanical part of systems, and also it may lead to instability.

In order to enhance the vehicle ride comfort using appropriate control scheme, an extended state observer based on (a-PIDSMC) in the present paper is proposed to get better performance for MR-damped quarter vehicle suspension system. Within the authors' best knowledge, this proposal is introduced for the first time in MR-damped vehicle suspension system. The proportional- integral-differential (PID) and extended state observer (ESO) are presented for estimation of unknown uncertain dynamics of the system. The unknown dynamics is bounded and the parameters of ESO are selected carefully to avoid non-null estimation error (Freidovich and Khalil, 2008). Regarding estimation error of ESO, a subsidiary sliding mode controller is supplied to the ESO based PID control in this paper. The proposed control scheme will be referred to as a-PIDSMC. By application of the Lyapunov stability theory, the stability of the proposed a-PIDSMC control is proved. The model is examined on two excitations: road bump and random road profile, using simulations generated by Matlab/Simulink software. The effectiveness of a-PIDSMC controller is compared with conventional SMC control proposed in reference (Zhang et al., 2015), conventional PID controller tuned according to Ziegler-Nichols method, MR passive and passive suspension system.

The rest of this article is arranged as follows: Section 2 gives a brief explanation of the MR damped vehicle. The algorithm is described in section 3. The results for two types of road disturbance inputs are demonstrated and discussed in section 4.

2. MODEL DESCRIPTION

2.1 Quarter-car suspension model

Dynamic model of a quarter car is established as shown in Fig. 1. The car body mass and the wheel mass are denoted by m_s and m_w , respectively; the vertical displacement of the

body and the wheel masses are represented by x_s and x_w , respectively; k_s and k_t are the spring and tyre stiffness, respectively; Assuming the motion only in vertical plane motion and neglecting other motions such as roll and pitch, the dynamic equations of the model are derived as

$$m_s \ddot{x}_s + k_s (x_s - x_w) + f_R = 0 \quad (1)$$

$$m_w \ddot{x}_w - k_s (x_s - x_w) + k_t (x_w - x_r) - f_R = 0 \quad (2)$$

The damping force f_R is given by

$$f_R = \begin{cases} c_s (\dot{x}_s - \dot{x}_w), & \text{for passive suspension.} \\ f_a, & \text{for semi-active suspension.} \end{cases} \quad (3)$$

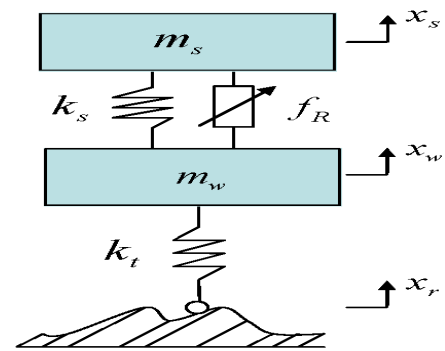


Fig. 1. A quarter-car structure with semi-active suspension.

The damping force f_a depends on the desired force generated by the system controller. The parameter values of the vehicle suspension model are taken from (Choi et al., 2000) as listed in Table 1.

The road excitation x_r and damping force f_R are selected as input vector. Taking dynamics relationship into account, the state variables can be defined as

$$x = [x_s \ x_w \ \dot{x}_s \ \dot{x}_w]^T \quad (4)$$

Referring to (1) and (2), a state-space representation can be derived as

$$\dot{x} = Ax + Bu \quad (5)$$

$$y = Cx + Du \quad (6)$$

Where

$$A = \begin{bmatrix} 0 & 0 & 1 & 0 \\ 0 & 0 & 0 & 1 \\ -\frac{k_s}{m_s} & \frac{k_s}{m_s} & -\frac{c_s}{m_s} & \frac{c_s}{m_s} \\ \frac{k_s}{m_w} & -\frac{(k_s + k_t)}{m_w} & \frac{c_s}{m_w} & -\frac{c_s}{m_w} \end{bmatrix},$$

$$B = \begin{bmatrix} 0 & 0 \\ 0 & 0 \\ 0 & -\frac{1}{m_s} \\ \frac{k_t}{m_w} & \frac{1}{m_w} \end{bmatrix}, \text{ and } u = \begin{bmatrix} x_r \\ f_R \end{bmatrix}.$$

$$C = \begin{bmatrix} 1 & 0 & 0 & 0 \\ 0 & 1 & 0 & 0 \\ 1 & -1 & 0 & 0 \\ 0 & 0 & 1 & 0 \end{bmatrix}, D = \begin{bmatrix} 0 & 0 \\ 0 & 0 \\ 0 & 0 \\ 0 & 0 \end{bmatrix}$$

Table 1. Parameter values of the quarter car suspension model (Choi et al., 2000).

Parameter	m_s (kg)	m_w (kg)	k_s (N/m)	k_t (N/m)	C_s (Ns/m)
Value	375	29.5	20580	200,000	772

2.2 MR-damper model

The modified Bouc-wen model described by (Dyke et al., 1996), shown in Fig. 2 which is widely used for modelling hysteretic systems, has been selected for the study of the MR-damper. In Fig. 2, y represents the internal moment of the MR-damper, u is the output signal from the first-order filter. k_1 represents the accumulator stiffness. c_0 , and c_1 represent the viscous damping coefficients detected at high and low damper velocities, respectively. Also x_0 is used to simulate the effect of the MR damper accumulator.

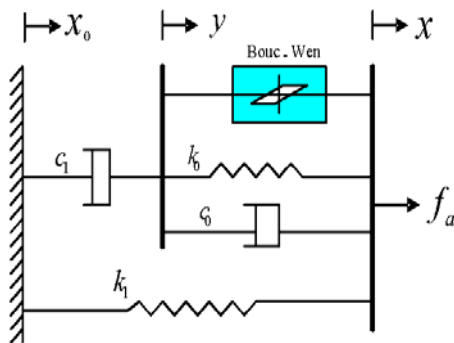


Fig. 2. The modified Bouc-wen model.

The governing equations for the equilibrium of forces on the rigid bar can be written as

$$c_1 \dot{y} = \alpha z + c_0 (\dot{x} - \dot{y}) + k_0 (x - y) \quad (7)$$

The shape and the scale of the hysteretic effect of the MR-damper can be predicted by γ , β , A and η . Variable z is an evaluation parameter to grant the hysteretic behaviour and is defined as

$$\dot{z} = -\gamma |\dot{x} - \dot{y}| |z|^{n-1} z - \beta (\dot{x} - \dot{y}) |z|^n + A (\dot{x} - \dot{y}) \quad (8)$$

Equation (7) can be rewritten as

$$\dot{y} = \frac{1}{c_0 + c_1} \{ \alpha z + c_0 \dot{x} + k_0 (x - y) \} \quad (9)$$

The total force generated by the system is then calculated by summation of the forces on upper and lower parts of the model expressed in Fig.2, yielding

$$f_a = \alpha z + c_0 (\dot{x} - \dot{y}) + k_0 (x - y) + k_1 (x - x_0) = c_1 \dot{y} + k_1 (x - x_0) \quad (10)$$

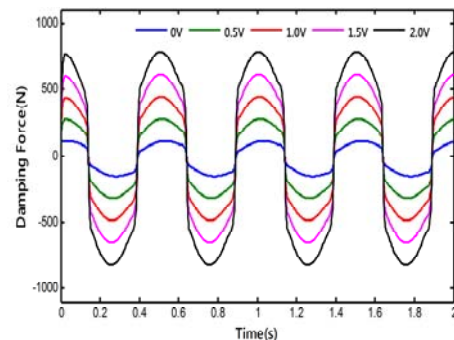
The effect of magnetic field arising from voltage applied to windings of the MR-damper can be described as

$$\left. \begin{aligned} \alpha &= \alpha(q) = \alpha_a + \alpha_b q \\ c_1 &= c_1(q) = c_{1a} + c_{1b} q \\ c_0 &= c_0(q) = c_{0a} + c_{0b} q \end{aligned} \right\} \quad (11)$$

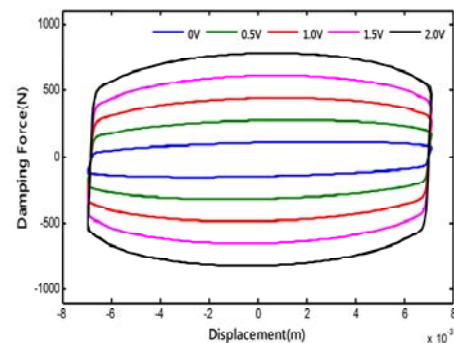
Denoting the applied voltage as v , the output voltage signal from the first-order filter q is written as

$$\dot{q} = -\eta(q - v) \quad (12)$$

To explain the behaviour of the modified Bouc-Wen model MR-damper the parameters values used are listed in Table 2 as utilized in reference (Metered et al., 2010). Hysteresis behaviour of the MR-fluid damper is demonstrated in Figs. 3, where a displacement of 0.007m amplitude and 2Hz frequency is applied to the MR-damper, and the voltage is applied as 0, 0.5, 1.0, 1.5 and 2V, respectively.



(a)



(b)

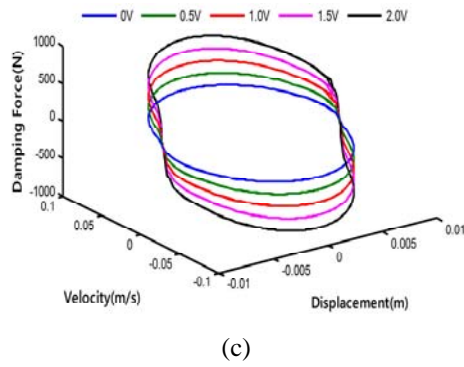


Fig. 3. Damping force versus (a) time, (b) displacement, (c) velocity and displacement.

Table 2. Modified Bouc-Wen model parameters as in
(Metered et al., 2010).

Symbol	Value (Unit)	Symbol	Value (Unit)
c_{0a}	784 (Ns / m)	α_a	12441 (N / m)
c_{0b}	1803 (Ns / Vm)	α_b	38430 (N / Vm)
k_0	3610 (N / m)	γ	136320 (m ⁻²)
c_{1a}	14649 (Ns / m)	β	2059020 (m ⁻²)
c_{1b}	34622 (Ns / Vm)	A	58
k_1	840 (N / m)	n	2
x_0	0.0245 (m)	η	190 (s ⁻¹)

3. CONTROL ALGORITHM

The control block diagram of MR damped vehicle suspension system is depicted in Fig.4. As mentioned previously in the introduction, the whole control system consists of two controllers: a system controller that uses the dynamic responses of the plant to calculate the desired damping force f_d according to PID, SMC and a-PIDSMC controllers; and the damper controller that predicts the voltage v applied to the damper in order to track its actual force f_a to the desired force f_d . Equations (7-12) have to be used to estimate f_a and implemented along with equations (1-6). In order to ensure the ride comfort and vehicle stability, performance measure such as suspension working space (SWS), vertical body acceleration (BA) and dynamic tyre load (DTL) are evaluated for all investigated systems under different road profiles. A brief description is provided in the following subsections.

3.1 Advanced proportional-integral-differential sliding mode control

In this part, the principle of a-PID and a-PIDSMC is introduced. The a-PIDSMC in closed-loop system stability is proved.

3.1.1 Advanced proportional-integral-differential part

For general nonlinear system with single input $u(t)$ and single output $y(t)$, if the derivative order of the system is

L where $L \geq 1$, input gain is μ , and $F(t)$ represents the disturbance of lumped unknown dynamics then the Ultra-local model can be defined as

$$y^{(L)}(t) = F(t) + \mu u(t) \quad (13)$$

According to (Wang et al., 2016), if $L = 1$, y^* is the desired reference, $e = y^* - y$ is the output error and k_p, k_i and k_d are the proportional, integral and derivative coefficients, respectively. The proposed PID is defined as

$$u = \frac{1}{\mu} (-F + \dot{y}^* + k_p \cdot e + k_i \int e \cdot dt + k_d \frac{de}{dt}) \quad (14)$$

Substituting (14) into (13), the closed loop system error equation can be obtained as

$$\dot{e} + k_p \cdot e + k_i \int e \cdot dt + k_d \frac{de}{dt} = 0 \quad (15)$$

The values of the parameters k_p, k_i and k_d can be selected by Hurwitz criterion.

If the estimation error is considered, the input can be rewritten as

$$u = \frac{1}{\mu} (-\hat{F} + \dot{y}^* + k_p \cdot e + k_i \int e \cdot dt + k_d \frac{de}{dt}) \quad (16)$$

An extended state observer (ESO) method is to be used in this work to estimate disturbance \hat{F} . Defining z_1, z_2 are the ESO states; z_3 is the extended state estimate; i.e. $z_3 = \hat{F}$; e_1 is the observing error; β_1, β_2 and β_3 are the observer gains. According to ESO method for estimating both the states and the extended state for the uncertain system can be given as follows (Yang and Huang, 2009).

$$\begin{cases} \dot{z}_1 = z_2 - \beta_1 \text{fal}(e_1, \alpha_1, \delta) \\ \dot{z}_2 = z_3 - \beta_2 \text{fal}(e_1, \alpha_2, \delta) \\ \dot{z}_3 = -\beta_3 \text{fal}(e_1, \alpha_3, \delta) \end{cases} \quad (17)$$

and

$$\text{fal}(e, \alpha, \delta) = \begin{cases} |e|^\alpha \text{sgn}(e) & \text{if } |e| > \delta, 0 \leq \alpha \leq 1 \text{ and } \delta > 0. \\ e / \delta^{1-\alpha} & \text{otherwise.} \end{cases}$$

Defining the disturbance error estimated by observer as $\tilde{F} = F - \hat{F}$, and considering $L = 1$, in equation (13), then implementing (16) into (13), the error equation is obtained as

$$\dot{e} + k_p \cdot e + k_i \int e \cdot dt + k_d \frac{de}{dt} + \tilde{F} = 0 \quad (18)$$

From reference (Freidovich and Khalil, 2008), one has generally $\|\tilde{F}\| \leq f_m$ with f_m an upper bound value.

Applying Laplace transformation method to (18), one can obtain

$$(s + k_p + \frac{k_i}{s} + k_d s)E(s) + \tilde{F}(s) - \tilde{F}(0) = 0 \quad (19)$$

let $k_d' = 1 + k_d$, the steady state error can be calculated as

$$e(t_\infty) = \lim_{t \rightarrow \infty} e(t) = \lim_{s \rightarrow 0} \frac{(1/k_d')s}{s^2 + (k_p/k_d')s + k_i/k_d'} (\tilde{F}(0) - \tilde{F}(s)) \quad (20)$$

where the steady state error $e(t_\infty)$ is ensured to tend to zero, and the performance of PID depends on the values of gains k_p, k_i, k_d and the estimated value of F .

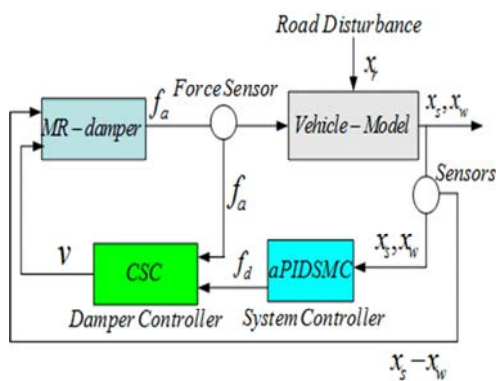


Fig. 4. MR-damped vehicle semi-active suspension control block diagram.

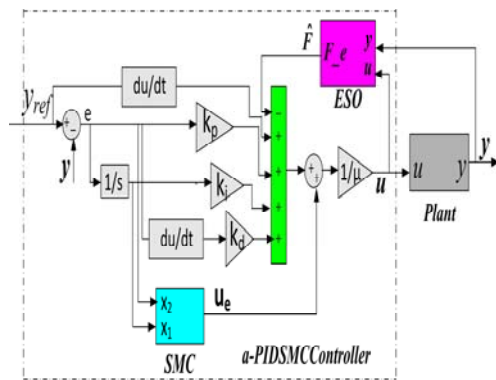


Fig. 5. a-PIDSMC controller block diagram.

3.1.2 Advanced proportional-integral-derivative sliding mode part

In this part, an extra component is added to the input to compensate the estimation error. The extra component is defined as u_e . The block diagram of advanced proportional-integral-derivative sliding mode controller (a-PIDSMC) is shown in Fig.5. The final input of a-PIDSMC controller is

$$u = \frac{1}{\mu} (-\hat{F} + \dot{y}^* + k_p \cdot e + k_i \int e \cdot dt + k_d \frac{de}{dt}) + u_e \quad (21)$$

Treating ultra-local model as first order ($L=1$) and substituting (21) into (13), resulting in the closed-loop error deduced as

$$\dot{e} + k_p \cdot e + k_i \int e \cdot dt + k_d \frac{de}{dt} + \mu u_e + \tilde{F} = 0 \quad (22)$$

Defining x_1 and x_2 as follows:

$$\begin{cases} x_1 = \int e \cdot dt \\ x_2 = e \end{cases} \quad (23)$$

Referring to (22) and (23), and put $k_d' = 1 + k_d$, one can obtain

$$\begin{cases} \dot{x}_1 = x_2 \\ \dot{x}_2 = -(k_p x_2 + k_i x_1 + \mu u_e + \tilde{F}) / k_d' \end{cases} \quad (24)$$

The extra input component u_e is designed to compensate the disturbance. Therefore, using a slide mode framework by defining a switching function S as

$$S = x_2 + c x_1 \quad (25)$$

Hence the derivative of (25) is

$$\dot{S} = (c - k_p / k_d') x_2 - (k_i x_1 + \mu u_e + \tilde{F}) / k_d' \quad (26)$$

The extra input component u_e contains two parts:

- equivalent control signal u_1 which ensures the ideal sliding mode condition ($\dot{S} = 0$); and
- correction control signal u_2 which reduce the chattering effects.

To ensure the stability of the closed-loop system, the input should be selected in such a way that state trajectories are confined to the sliding hyper surface.

Thus putting the extra input as

$$u_e = u_1 + u_2 \quad (27)$$

In order to calculate the ideal sliding mode condition u_1 , replace \tilde{F} with f_m in (26) yields

$$u_1 = \frac{1}{\mu} ((c k_d' - k_p) x_2 - k_i x_1 - f_m) \quad (28)$$

For reducing the chattering effects, u_2 is selected as

$$u_2 = \frac{1}{\mu} (\eta_1 \text{sat}(S, \varepsilon) + \eta_2 S) \quad (29)$$

where

$$\text{sat}(S, \varepsilon) = \begin{cases} 1 & , S > \varepsilon \\ S/\varepsilon & , \|S\| \leq \varepsilon \text{ and } \eta_1 > 0, \eta_2 > 0, \varepsilon > 0. \\ -1 & , S < -\varepsilon \end{cases}$$

3.1.3 Proof Stability

The stability can be proved by choosing the Lyapunov function in the following form

$$V(t) = \frac{1}{2} S^2 \quad (30)$$

By calculating the derivative of $V(t)$ then,

$$\begin{aligned} \dot{V}(t) &= \dot{S} \\ &= S(((c - k_p / k_d')x_2 - (k_i x_1 + \mu u_e + \tilde{F}) / k_d')) \\ &= S(((c - k_p / k_d')x_2 - (k_i x_1 + \mu(u_1 + u_2) + \tilde{F}) / k_d')) \\ &= -S(\eta_1 \text{sat}(S, \varepsilon) + \eta_2 S + \tilde{F} - f_m) / k_d' \end{aligned} \quad (31)$$

Once $\|\tilde{F}\| \leq f_m$ with f_m an upper bound value, if $S < -\varepsilon$, the boundaries of \tilde{F} are sufficient to satisfy $\dot{V}(t) = -S(-\eta_1 + \eta_2 S + \tilde{F} - f_m) < 0$. If $S > \varepsilon$, to ensure that $\dot{V}(t) < 0$ if one has $\eta_1 > 2f_m$, $\dot{V}(t) = -S(\eta_1 + \eta_2 S + \tilde{F} - f_m) < 0$. since \tilde{F} is bounded.

If $|S| < \varepsilon$, one can obtain

$$\dot{V}(t) = -S(\eta_1 S / \varepsilon + \eta_2 S + \tilde{F} - f_m) \quad (32)$$

The condition to ensure the negative right-side term is

$$-S(\tilde{F} - f_m) - (\eta_2 + \eta_1 / \varepsilon) S^2 < 0 \quad (33)$$

Again since \tilde{F} is bounded and $|S| < \varepsilon$, the stable condition is $(\varepsilon \eta_2 + \eta_1) > 2f_m$.

Therefore, the conditions need to prove the stability are $\eta_1 > 2f_m$ and $\eta_2 > 0, \varepsilon > 0$.

3.2 Damper controller

The continuous-state control was employed by (Metered et al., 2010) and (Lam and Liao, 2003) to estimate the voltage applied to the MR Damper's coil. The response of the MR damper could be linearized by feedback control method. The desired force compared to the MR damper's actual force which fed back with a gain H . The resultant error is scaled by a gain G . To make sure the damper cannot produce energy to the system, the controller function is enabled strictly when the direction of damping force and also the error have the same direction. Therefore, it is essential to have a sign correction. If they have different sign, the input voltage has to be set zero. Representing the control force

determined by the system controller as f_d . The variation of required control signal is ranges between the maximum voltage V_{\max} , and minimum voltage V_{\min} . The input voltage is obtained using continuous state method and may be stated as

$$v = \begin{cases} V_{\max}, & \varphi > V_{\max} \\ V_{\min}, & \varphi < V_{\min} \\ \varphi, & \text{Otherwise} \end{cases} \quad (34)$$

where

$$\varphi = G(f_d - Hf_a) \text{sgn}(f_a)$$

The values of G and H are decided by trial-and-error method. In this paper, the values of G , H and V_{\max} are set to be $0.0038V/N$, 1 and $2V$, respectively, as in reference (Lam and Liao, 2003).

4. RESULTS AND DISCUSSION

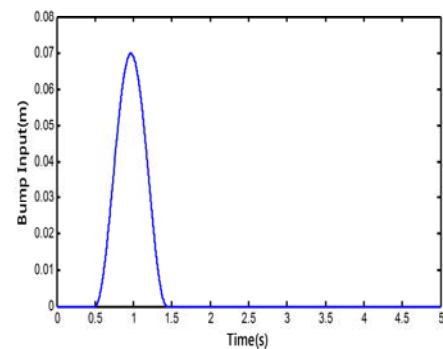
The vertical body acceleration (BA), and dynamic tire load (DTL) are two frequently-used assessment criteria on riding comfort and handling stability of vehicle, meanwhile, the suspension working space (SWS) affects the running performance of vehicle to some extent (Rajesh, 2006).

The effectiveness of the proposed semi-active suspension using a-PIDSMC controller, is compared with the performance of SMC, PID controller, conventional passive suspension system with damping constant of $c_s = 772Ns/m$ as in (Choi et al., 2000) and MR Passive suspension.

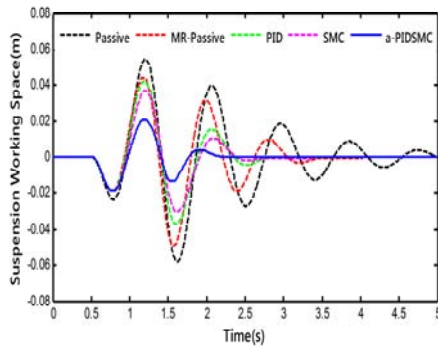
Two types of road excitation were selected in this study. The first excitation is a road bump and represented by (Choi and Kim, 2000) as:

$$x_r = \begin{cases} a(1 - \cos(\omega_r(t - 0.5))), & \text{for } 0.5 \leq t \leq 0.5 + d_b / V_c \\ 0, & \text{otherwise} \end{cases} \quad (35)$$

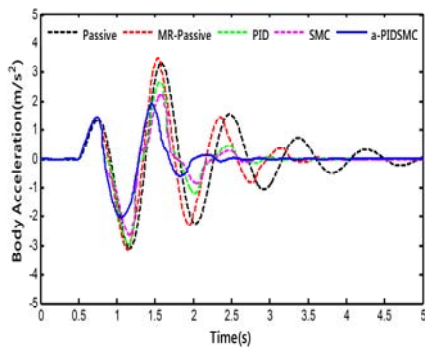
where a is the half of bump amplitude, $\omega_r = 2\pi V_c / d_b$, d_b is the bump width and V_c is the bump velocity. The parameter values of a , d_b and V_c are $0.035m$, $0.8m$ and $0.856m/s$ respectively as in (Choi and Kim, 2000).



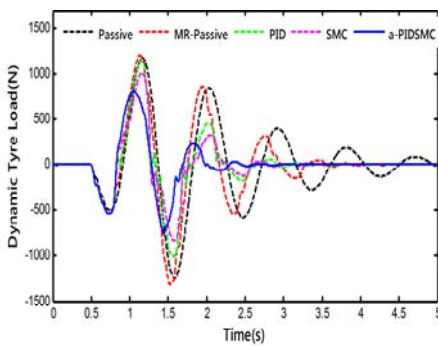
(a)



(b)



(c)



(d)

Fig. 6. The time response of the system under excitation of the road bump. (a) Road displacement, (b) SWS, (c) BA, (d) DTL.

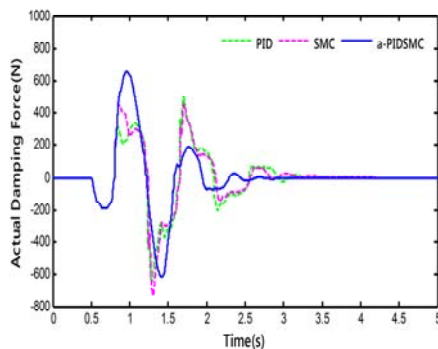


Fig. 7. Comparison of actual damping force under road bump

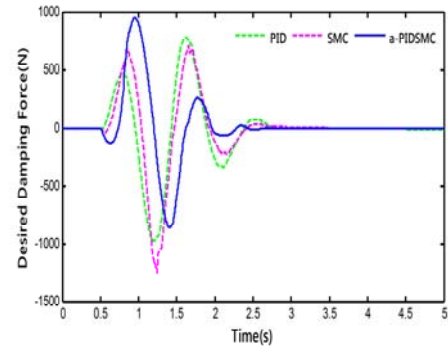


Fig. 8. Comparison of desired damping force under road bump.

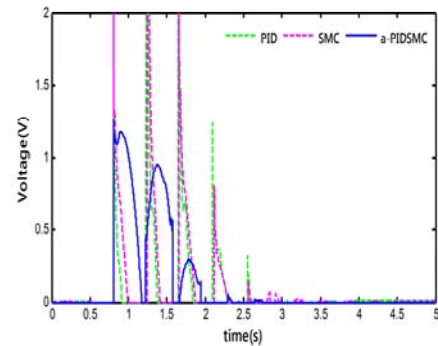


Fig. 9. Comparison of input voltage under road bump.

Under bump excitation, the displacement of the road input signal is shown in Fig.6 (a).The time histories of the SWS, BA, and DTL responses under this road disturbance excitation are illustrated in Figs. 6(b-d), respectively. For controlled semi-active suspension in the case of PID, SMC and a-PIDSMC controller, the comparison of the actual damping control force generated by MR damper is provided in Fig. 7, the desired force generated by controllers is shown in Fig. 8, and the input control voltage for different controllers is supplied in Fig. 9. It can be concluded from Figs. 7 and 8, that the damper control force and the desired control force show the similar variation trend, which means that the modified Bouc-wen model of MR damper can precisely track the desired control force .According to Fig. 9, the input voltage signal in the case of a-PIDSMC controller is relatively continuous and smooth. Conversely, the maximum value of the input voltage in the controlled system by PID and SMC controller is higher than in the case of a-PIDSMC controller.

Figs. 6(b-d), show the comparison of the controlled semi-active using a-PIDSMC with SMC controller, PID controller, MR Passive suspension and conventional passive suspension systems. The peak-to-peak (PTP) values of the system response and their improvements percentages are recorded in Tables.3 (a-c). From these results, it is clearly seen that the SWS of semi active suspension system controlled by a-PIDSMC is decreased by 61.95%, 53.27%, 50.71% and 43.90% compared with semi active suspension system controlled by SMC controller, PID controller, MR Passive and conventional passive, respectively. The BA is decreased

by 41.03%, 44.08%, 26.56% and 11.94%, respectively. The DTL is decreased 31.51%, 32.94%, 29.48% and 19.82% respectively. Thus semi-active vehicle suspension system controlled using a-PIDSMC offers a superior performance.

Moreover, to validate the effectiveness of a-PIDSMC controller, a second type of road excitation, is a random road excitation. The random road input model is gained by integration of white-noise signal. The frequency spectrum density formula of the road form in the time domain as described by(Wang et al., 2015).

$$G_q(f) = \frac{1}{v} G_q(n_0) \left(\frac{n}{n_0}\right)^{-2} = G_q(n_0) n_0^2 \frac{v}{f^2} \quad (36)$$

where $G_q(n_0)$ is the road roughness coefficient. v is the vehicle speed. f is the frequency in time domain. n is the space frequency, and it represents per meter length of the wave number. $n_0 = 0.1m^{-1}$, is the space frequency reference value. The power spectrum function $G_q(f)$ of vehicle speed in the time domain can be expressed by

$$G_q(f) = (2\pi f)^2 \cdot G_q(n) = 4\pi^2 G_q(n_0) n_0^2 v \quad (37)$$

If vehicle speed is assumed to be constant, $G_q(f)$ can be calculated, and it is denoted by C_n . Hence, the road input can be described as follows

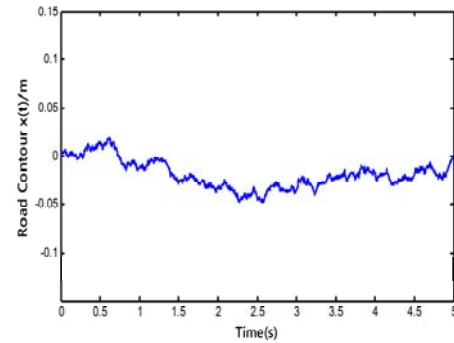
$$x(t) = C_n^{1/2} \int_t w(t) dt \quad (38)$$

where $w(t)$ is white-noise. If letting the speed is 20 m/s and the road is B rank, it can be obtained that $G_q(n_0) = 64 \times 10^{-6}$, $C_n = 5.05 \times 10^{-4}$. Thus, the formula (38) can be given by

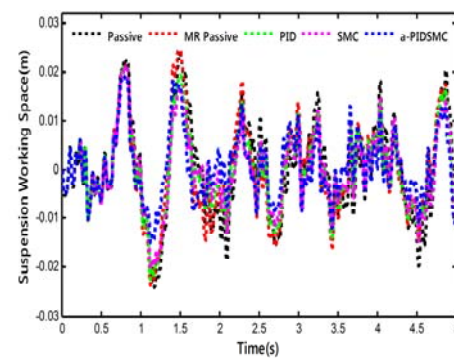
$$x(t) = 0.0225 \int_t w(t) dt \quad (39)$$

For the quarter car vehicle model under the random road excitation, the displacement of the road input signal is shown in Fig.10 (a). The time histories of SWS, DTL and BA are presented in Figs.10 (b-d), respectively. Meanwhile, in the cases of PID, SMC and a-PIDSMC controller, the comparison of the actual damping control force, the desired control force and the input control voltage for MR damper are provided in Figs. 11-13. The simulation results for these cases to be additional prove the validity of the modified Bouc-wen model of MR-damper. The relevant root mean square (RMS) values of SWS, BA, and DTL for semi-active suspension system controlled by a-PIDSMC compared with SMC controller, PID controller, MR Passive suspension and conventional passive suspension systems. The results are presented in Tables.4 (a-c). The SWS is reduced 31.31%, 25.27%, 13.92% and 8.11% respectively. BA is reduced by 0.44%, 15.00%, 9.78% and 8.90%, respectively. The BA reductions are not obvious due to contradiction between the ride comfort and handling stability control. DTL is reduced by 21.42%, 22.08%, 19.56% and 18.47%, respectively. Typically, it can be remarked from Table.4, that the proposed

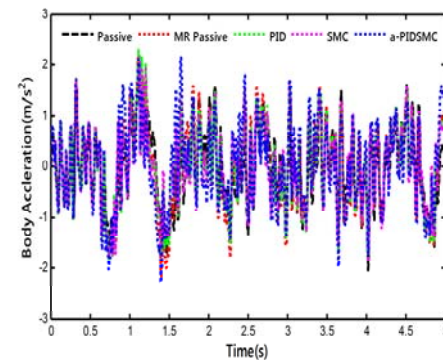
a-PIDSMC controller has over all good performance as compared to conventional passive, MR Passive, PID controlled and SMC controlled suspension system.



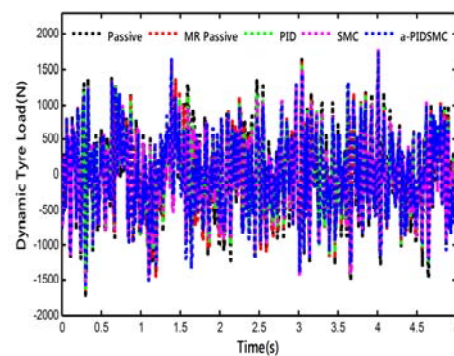
(a)



(b)



(c)



(d)

Fig.10. The time response of the system under random road input. (a) Road displacement, (b) SWS, (c) BA, (d) DTL.

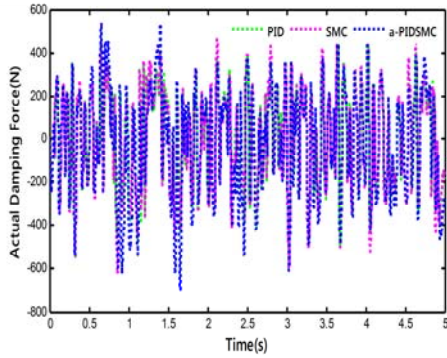


Fig. 11. Comparison of actual damping force under random road excitation.

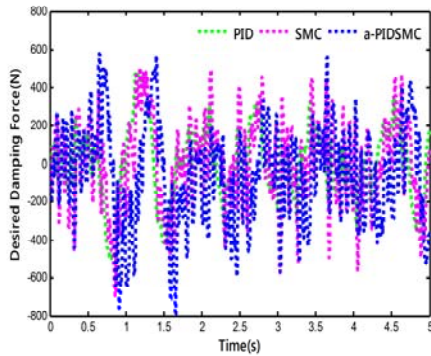


Fig. 12. Comparison of desired damping force under random road disturbance.

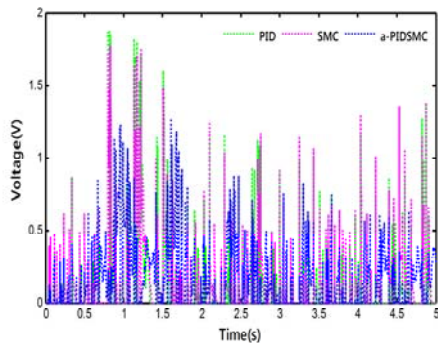


Fig. 13. Comparison input voltage under random road excitation.

5. CONCLUSIONS

In this paper, an advanced proportional-integral-derivative sliding mode control (a-PIDSMC) has been proposed for semi-active MR-damped quarter vehicle suspension system to improve vehicle ride comfort and stability. Dynamic model of MR damped quarter-vehicle was performed and simulated using Matlab/Simulink software. The system controller is designed using a-PIDSMC, while for the damper controller; the continuous state control is applied. The effectiveness of the proposed a-PIDSMC controller have been demonstrated and compared with conventional SMC, along with classic PID controller tuned according to Ziegler-Nichols method, MR, and passive suspension systems. Simulation results indicate that the proposed control system minimizes the

suspension working space; body acceleration and dynamic tire load in an effective manner and thus improves the ride comfort and ride safety of the vehicle. The a-PIDSMC controller does not depend on the system modelling. The proposed scheme can be further improved using Particle Swarm Optimization (PSO) for tuning PID parameters.

Table 3(a). Peak to peak (PTP) values of SWS for the road bump input.

System Type	SWS (m)	% Imp Respect to Passive	% Imp Respect to MR Passive	% Imp Respect to PID	% Imp Respect to SMC
Passive	0.0544	---	---	---	---
MR Passive	0.0443	18.57	---	---	---
PID	0.0420	22.79	5.19	---	---
SMC	0.0369	32.17	16.70	12.14	---
a-PIDSMC	0.0207	61.95	53.27	50.71	43.90

Table 3(b). Peak to peak (PTP) values of BA for the road bump input.

System Type	BA (m/s ²)	% Imp Respect to Passive	% Imp Respect to MR Passive	% Imp Respect to PID	% Imp Respect to SMC
Passive	3.3115	---	---	---	---
MR Passive	3.4923	-5.46	---	---	---
PID	2.6593	19.70	23.85	---	---
SMC	2.2176	33.03	36.50	16.61	---
a-PIDSMC	1.9529	41.03	44.08	26.56	11.94

Table 3(c). Peak to peak (PTP) values of DTL for the bump disturbance.

System Type	DTL (N)	% Imp Respect to Passive	% Imp Respect to MR Passive	% Imp Respect to PID	% Imp Respect to SMC
Passive	1177.33	---	---	---	---
MR Passive	1202.46	-2.13	---	---	---
PID	1143.38	2.88	4.91	---	---
SMC	1005.73	14.58	16.36	12.04	---
a-PIDSMC	806.34	31.51	32.94	29.48	19.82

Table 4(a). Root mean square (RMS) values of SWS for the random road disturbance.

System Type	SWS (m)	% Imp Respect to Passive	% Imp Respect to MR Passive	% Imp Respect to PID	% Imp Respect to SMC
Passive	0.0099	---	---	---	---
MR Passive	0.0091	8.08	---	---	---
PID	0.0079	20.20	13.19	---	---
SMC	0.0074	25.25	18.68	6.33	---
a-PIDSMC	0.0068	31.31	25.27	13.92	8.11

Table 4(b). Root mean square (RMS) values of BA for the random road excitation.

System Type	BA (m/s ²)	% Imp Respect to Passive	% Imp Respect to MR Passive	% Imp Respect to PID	% Imp Respect to SMC
Passive	0.7424	---	---	---	---
MR Passive	0.8695	-17.12	---	---	---
PID	0.8192	-10.34	5.78	---	---
SMC	0.8113	-9.28	6.69	0.96	---
a-PIDSMC	0.7391	0.44	15.00	9.78	8.90

Table 4(c). Root mean square (RMS) values of DTL for the random road disturbance

System Type	DTL (N)	% Imp Respect to Passive	% Imp Respect to MR Passive	% Imp Respect to PID	% Imp Respect to SMC
Passive	582.42	---	---	---	---
MR Passive	587.36	-0.85	---	---	---
PID	568.93	2.31	3.14	---	---
SMC	561.30	3.63	4.44	1.34	---
a-PIDSMC	457.64	21.42	22.08	19.56	18.47

ACKNOWLEDGEMENT

This research has been supported by Natural Science Foundation of China Government, Grant No. (11472135) and Science Challenge Project, Grant No. (JCKY2016212A506-0104). This support is gratefully acknowledged.

REFERENCES

- Choi, S.-B. & Kim, W.-K. (2000). Vibration control of a semi-active suspension featuring electrorheological fluid dampers. *Journal of Sound and vibration*, 234, 537-546.
- Choi, S., Choi, Y. T. & Park, D. (2000). A sliding mode control of a full-car electrorheological suspension system via hardware in-the-loop simulation. *Transactions-american society of mechanical engineers journal of dynamic systems measurement and control*, 122, 114-121.
- Dyke, S., Spencer JR, B., Sain, M. & Carlson, J. (1996). Modeling and control of magnetorheological dampers for seismic response reduction. *Smart materials and structures*, 5, 565.
- Freidovich, L. B. & Khalil, H. K. (2008). Performance recovery of feedback-linearization-based designs. *IEEE Transactions on automatic control*, 53, 2324-2334.
- Gad, S., Metered, H., Bassuiny, A. & Ghany, A. A. (2015). Vibration Control of Semi-active MR Seat Suspension for Commercial Vehicles Using Genetic PID Controller. *Vibration Engineering and Technology of Machinery*. Springer.
- Guo, D., Hu, H. & Yi, J. (2004). Neural network control for a semi-active vehicle suspension with a magnetorheological damper. *Modal Analysis*, 10, 461-471.
- Hu, G., Liu, Q., Ding, R. & Li, G. (2017). Vibration control of semi-active suspension system with magnetorheological damper based on hyperbolic tangent model. *Advances in Mechanical Engineering*, 9, 1687814017694581.
- Karkoub, M. A. & Zribi, M. (2006). Active/semi-active suspension control using magnetorheological actuators. *International journal of systems science*, 37, 35-44.
- Kaya, I. (2007). Sliding-mode control of stable processes. *Industrial & engineering chemistry research*, 46, 571-578.
- Lam, A. H.-F. & Liao, W.-H. (2003). Semi-active control of automotive suspension systems with magnetorheological dampers. *International Journal of Vehicle Design*, 33, 50-75.
- Liao, W. & Wang, D. (2003). Semiactive vibration control of train suspension systems via magnetorheological dampers. *Journal of intelligent material systems and structures*, 14, 161-172.
- Lin, J.-S. & Kanellakopoulos, I. Nonlinear design of active suspensions. *Decision and Control*, (1995), Proceedings of the 34th IEEE Conference on, 1995. IEEE, 3567-3569.
- Metered, H., Bonello, P. & Oyadiji, S. (2010). An investigation into the use of neural networks for the semi-active control of a magnetorheologically damped vehicle suspension. *Proceedings of the Institution of Mechanical Engineers, Part D: Journal of Automobile Engineering*, 224, 829-848.
- Nugroho, P. W., Li, W., Du, H., Alici, G. & Yang, J. (2014). An adaptive neuro fuzzy hybrid control strategy for a semiactive suspension with magneto rheological damper. *Advances in Mechanical Engineering*, 6, 487312.
- Rajagopal, K. & Ponnusamy, L. 2014. Biogeography-based optimization of PID tuning parameters for the vibration control of active suspension system. *Journal of Control Engineering and Applied Informatics*, 16, 31-39.
- Rajesh, R. (2006). Vehicle dynamics and control. *Mechanical engineering series*. Springer, 257-285.
- Shehata, A., Metered, H. & Oraby, W. A. (2015). Vibration control of active vehicle suspension system using fuzzy logic controller. *Vibration Engineering and Technology of Machinery*. Springer.
- Wang, H., Li, S., Tian, Y. & Aitouche, A. (2016). Intelligent Proportional Differential Neural Network Control for Unknown Nonlinear System. *Studies in Informatics and Control*, 25, 445-452.
- Wang, W., Song, Y., Xue, Y., Jin, H., Hou, J. & ZHAO, M. (2015). An optimal vibration control strategy for a vehicle's active suspension based on improved cultural algorithm. *Applied Soft Computing*, 28, 167-174.
- Williams, R. (1994). Electronically controlled automotive suspensions. *Computing & Control Engineering Journal*, 5, 143-148.
- Wright, P. (1984). The application of active suspension to high performance road vehicles. *I Mech E Paper C239*, 123.

- Yang, X. & Huang, Y. Capabilities of extended state observer for estimating uncertainties. American Control Conference, 2009. ACC'09., (2009). IEEE, 3700-3705.
- Yang, Z., Zhang, J., Chen, Z. & Zhang, B. (2011). Semi-active control of high-speed trains based on fuzzy PID control. *Procedia Engineering*, 15, 521-525.
- Yao, J., Jiao, Z., Ma, D. & Yan, L. (2014). High-accuracy tracking control of hydraulic rotary actuators with modeling uncertainties. *IEEE/ASME Transactions on Mechatronics*, 19, 633-641.
- Zhang, H., Wang, E., Zhang, N., MIN, F., SUBASH, R. & SU, C. (2015). Semi-active sliding mode control of vehicle suspension with magneto-rheological damper. *Chinese Journal of Mechanical Engineering*, 28, 63-75.
- Zhu, X., Jing, X. & Cheng, L. (2011). A magnetorheological fluid embedded pneumatic vibration isolator allowing independently adjustable stiffness and damping. *Smart Materials and Structures*, 20, 085025.